Progress In Electromagnetics Research C, Vol. 66, 97–107, 2016

Circularly Polarized 2 × 2 MIMO Antenna for WLAN Applications

Leeladhar Malviya, Rajib K. Panigrahi, and Machavaram V. Kartikeyan*

Abstract—A 2 × 2 circularly polarized (CP) MIMO antenna is proposed to resonate at 5.8 GHz IEEE 802.11 WLAN band for non-line of sight (NLOS) communication. The proposed design achieves circular polarization with two optimized 90° apart rectangular slots etched at the center of a truncated rectangular patch. The proposed MIMO covers 5.49–6.024 GHz frequency band. The achieved isolation between two ports is more than 33 dB. The gain at the 5.8 GHz resonant frequency is 5.34 dBi. The diversity performance in terms of gain, ECC, and MEG has been reported.

1. INTRODUCTION

Highly isolated or very low mutual coupling among the multiple input multiple output (MIMO) antenna elements is achieved via space isolation (diversity) and polarization isolation techniques. The first one is not always feasible due to maximization of space requirements, which in turn requires higher cost of making antennas. The second one is due to orthogonal polarization of electromagnetic waves, and is preferred in designs. One of the issues at the receiving end is that the possibility of receiving unequal signal gains was high, due to the polarization mismatches because of independent fading in indoor and outdoor environments. In line of sight communication (LOS) even with linearly polarized MIMO, the receiving antennas are able to receive unequal signal powers. The antenna that receives the least power, limits the diversity gain, which in turn lowers the signal to noise ratio (SNR). The circularly polarized (CP) MIMO eliminates the polarization mismatch effect and equally divides the power among receiving radiators. The CP antenna has focusing, anti-jamming, and anti-interference capabilities.

Basic mechanism to achieve circular polarization (CP) is discussed in detail in literature. The first approach of CP wave generation was projected on the feed application at the diagonal axis of a patch. The second approach of CP wave generation depended on the perturbation of patch in terms of either oppositely truncated corners or oppositely located corner slots with diagonal feeding. The third approach of CP wave generation was based on a 45° diagonal slot at the center with microstrip feed. In the fourth approach, a perturbation in a square slot with unequal L-shaped patch/ground arms [1] and asymmetric slits/slots are used to generate CP mode [2, 3].

The discussed approaches have been seen individually as well as jointly in different designs. In a design, a dual-excitation approach with dumbbell-shaped defected ground structure (DGS) was used for reconfigurability in beam steering, and improvement in front to back-lobe ratio (FBR) [4, 5]. To avoid the problem of narrow bandwidth a coplanar waveguide (CPW) was used for designing CP polarized rhombic antennas for radio receivers [6]. Different fractal designs [7, 8] were used to achieve certain performance metrices of CP antennas. Similarly, a focused antenna array with L-shaped slot helps in generating CP mode, when etched in an oppositely chopped inset feed patch [9]. A sequentially rotated slot antenna structure can generate CP polarized wave for maximum power transfer [10].

Received 19 May 2016, Accepted 9 July 2016, Scheduled 21 July 2016

* Corresponding author: Machavaram Venkata Kartikeyan (kartik@ieee.org).

The authors are with the Electronics and Communication Engineering Department, Indian Institute of Technology (IIT), Roorkee (U. K.)-247667, India.

Similarly, the surface wave controlling using shorting pins/posts [11, 12], frequency agility [13], and polarization matching are the effects of CP polarization [14]. The CP antennas are used in radio frequency identification (RFID) trans-receive systems [15], airborne systems [16], and in automobile engineering applications [17].

The effect of CP on MIMO can be accounted as an increase of diversity gain, throughput, data rate, and capacity [18]. Similarly, to broaden the bandwidth of the CP array, multiple layers of substrate are also required along with the feed structure to make all the elements to be 90° phase shifted with equal amplitudes [19], and high gain can be achieved [20]. The segmented circles with 90° phase coupling (polarizers or stubs) in each circle and with power divider is also a approach of MIMO CP antennas [21, 22]. A slotted array antenna with slits was also reported in literature to generate CP polarization [23]. A polygon-shaped radiator with L-shaped arm responds with the dual-band CP characteristics. The isolation improvement between the MIMO radiators is achieved by the ground separator and by the placement of radiators [24].

The proposed design achieves circular polarization by two optimized 90° apart rectangular slots etched at the center of a rectangular patch. The 90° phased slots also enhance the bandwidth of the antenna. The two orthogonal modes with 90° phase and equal amplitudes are excited by slots etched at the center of truncated rectangular patches to generate CP mode. A single microstrip feed at an appropriate location, eliminates the need of matching network, external polarizer and also reduces the overall size of the design. A two-arm feed mechanism is used for the proposed design to spread the total power among radiating elements. It consists of 50 Ω, 70.7 Ω, and 100 Ω microstrip transmission lines and is helpful in designing of 2×2 MIMO. In our design, a 2×2 MIMO antenna with CP polarization is proposed with more than 33 dB of isolation between radiating elements. The designed MIMO covers 5.8 GHz IEEE 802.11 WLAN standard. The proposed work is reported in four sections. Section 2 describes design concept and fabrication. Sections 3 and 4 explain experimental results and conclusion.

2. DESIGN STUDIES AND RESULTS

The proposed 2×2 MIMO antenna is designed with circular polarization to trans-receive signals with left/right-hand CP wave. The proposed 2-port MIMO antenna with 50 Ω ports is designed using computer simulation tool (CST) version 12.0 and fabricated on an FR4 dielectric substrate (thickness of 1.524 mm, permittivity of 4.4, and loss tangent of 0.025) of size $27.69 \times 97\,\text{mm}^2$. The particle swarm optimization (PSO) approach with min-max algorithm was set to achieve the best design goals for the desired band of operation and for required antenna parameters. The minimum return loss, high isolation (low mutual coupling), compact size, sufficient antenna gain, and specific WLAN application are the design guidelines behind the selection of the proposed antenna.

A single microstrip feed is designed for 1×2 combinations. The microstrip feed is selected here to avoid cutting of substrate and conductive layers (as used in coaxial feed structure), and also to control surface waves. The proposed design achieves circular polarization by the optimization of two 90° apart rectangular slots etched at the center of the rectangular patch. A full ground structure is selected in design along with a slot (width 1.5 mm) in the ground in between the power divider arms to avoid direct coupling between them, and a ground split of 0.5 mm is used between two ports to avoid sharing of common ground. The optimized dimensions are obtained here while setting the min-max algorithm with ±10% variation in set values. The best results were achieved after 2100 iterations and are shown in Table 1. The schematic view and fabricated MIMO antenna are shown in Fig. 1 and Fig. 2.

Table 1. Optimized values of considered parameters (mm).

Parameter	a	b	c	d	e	f	g	h	l (50 Ω)	w (50 Ω)	l (70.7 Ω)
Value	9.64	11.0	24.98	2.96	10.5	0.692	13.75	3.26	2.0	2.96	2.0
Parameter	i	j	k	l	m	n	o	p	w (70.7 Ω)	l (100 Ω)	w (100 Ω)
Value	8.12	0.74	27.69	1.5	16.5	0.5	27.69	97.0	1.58	26.12	0.694

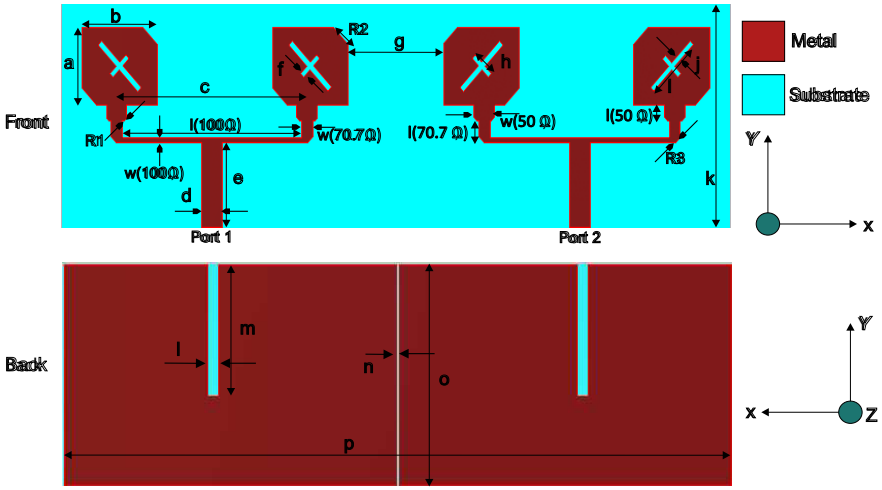

Figure 1. Schematic view of the proposed 2 × 2 CP MIMO antenna.

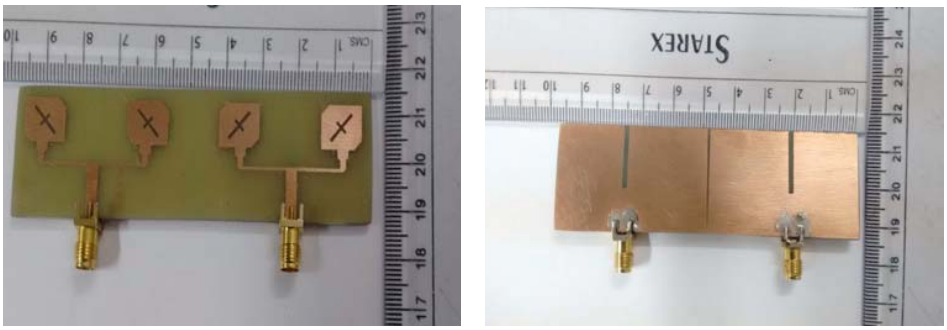

Front side Back side

Figure 2. Fabricated 2 × 2 CP MIMO antenna.

2.1. Simulation and Measurement Results

A calibrated two-port vector network analyzer (VNA)-HP8720B is used to test all the S parameters, and the far-field quantities are measured in an anechoic chamber for the validity of CST design and its simulated parameters.

A 2×2 CP MIMO is designed to solve the drawbacks of single elements, i.e., capacity, data rate, etc. The proposed 2 × 2 CP MIMO antenna with three cases of patch structures is shown in Fig. 3(a) and Fig. 3(b), for return loss, isolation and axial ratio (AR) characteristics. The first case of 2 × 2 MIMO antenna, with no slot in patch, has −10 dB impedance band of 5.82–5.994 GHz (bandwidth equals 174 MHz), and the corresponding value of isolation in the band is more than 35 dB. The MIMO antenna in this case is linearly polarized as the AR at the resonant frequency is 16.81 dB, and in frequency band AR is more than 10 dB. The MIMO antenna resonates at 5.908 GHz frequency.

The return loss in the first case was very close to −10 dB line. Therefore, the chopping of patch from the opposite corners and chopping of microstrip lines are considered for the next two cases to decrease the return loss. The second case of 2 × 2 MIMO antenna with one slot of 45° in patch has −10 dB impedance band of 5.548–6.076 GHz, and the corresponding value of isolation in the band is more than 33 dB. The MIMO antenna in this case is circularly polarized, as the AR at the resonant frequency of 5.85 GHz is 0.93 dB. A frequency shift of 672 MHz has been observed here in comparison with the first case, and the total bandwidth obtained here is 528 MHz. At 5.8 GHz frequency value of AR is 1.95. Such a single-slot approach was used in many of the described designs in literature.

In the third case, the proposed patch structure with 90° asymmetric slots is designed for better

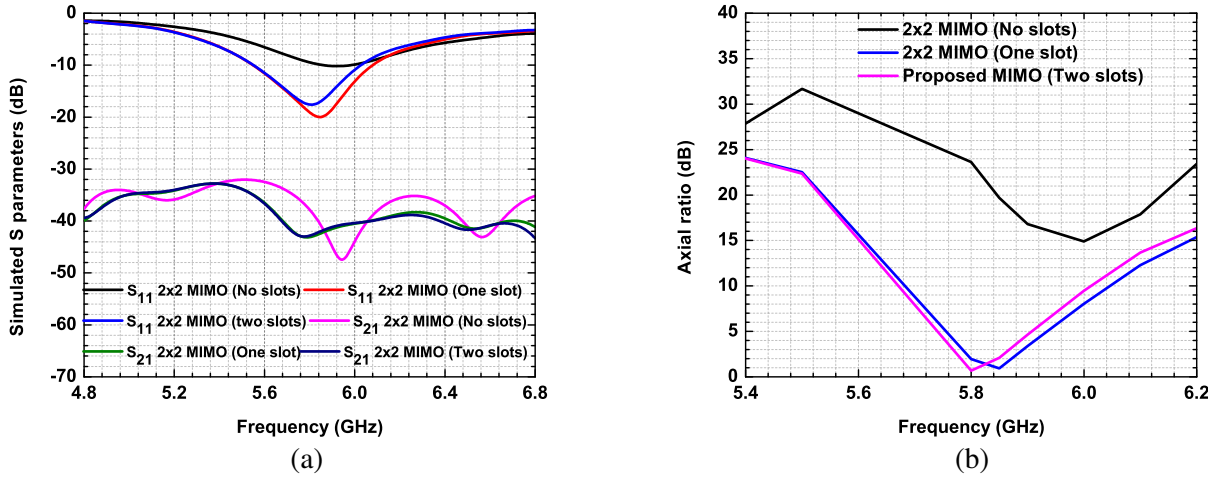

Figure 3. Comparison of simulated S parameters and axial ratio for different MIMO cases. (a) Simulated S parameters. (b) Simulated axial ratio.

Table 2. Comparison of MIMO (2×2) with different cases.

Antenna type	Frequency band (Simulated) GHz	Bandwidth (-10 dB) MHz	Resonant frequency (f_r) GHz	Isolation at f_r (dB)	Gain at f_r (dBi)
MIMO (2×2) with no slots in patch	5.82–5.994	174	5.91	44.75	5.38
MIMO (2×2) with one slot in patch	5.548–6.076	528	5.85	42.36	5.50
Proposed MIMO (2×2)	5.49–6.024	534	5.80	42.82	5.34

performance of AR characteristics than the patch with a single slot. The proposed 2×2 MIMO antenna with dual-slot in patch shows the CP polarization with -10 dB impedance band of 5.49–6.024 GHz, and the corresponding value of isolation is more than 33 dB. The bandwidth in this case is 534 MHz and is slightly higher than the second case. A 6 MHz of frequency shift towards lower frequency band is observed here in comparison with the second case. The proposed MIMO antenna resonates at 5.8 GHz frequency with AR value of 0.68 dB. The AR value in this case is much better than the second case. A slightly higher frequency band is the result of the second inclined slot in patch. A comparison of the considered cases are shown in Table 2.

Under the measurement state, unused ports are terminated by 50 Ω. It has been observed that CST MWS (CST microwave studio) and VNA results are in good agreement. From the simulation and measurement of S parameters, we find that $S_{11} = S_{22}$ and $S_{12} = S_{21}$. This situation exists due to the placement of two 1×2 single antennas in mirror positions. Therefore, for the simplicity of analysis, we consider S_{11} and S_{21} scattering parameters only, for plotting and measurement of other parameters throughout the paper.

Similarly, the measured and simulated S parameters are compared in Fig. 4(a). The simulated -10 dB impedance bandwidth extends from 5.49–6.024 GHz with more than 33 dB of in-band isolation. The MIMO antenna resonates at 5.8 GHz frequency with 42.82 dB of isolation and AR value of 0.68 dB. The simulated 3 dB AR band extends from 5.772–5.864 GHz (AR bandwidth equals 92 MHz), and provides gain of 5.34 dBi. Similarly, the measured -10 dB impedance bandwidth extends from 5.56–6.01 GHz with more than 34 dB of in-band isolation. The fabricated MIMO antenna resonates at 5.8 GHz frequency with 40.95 dB of isolation and AR value of 0.98 dB. The measured 3 dB AR band extends from

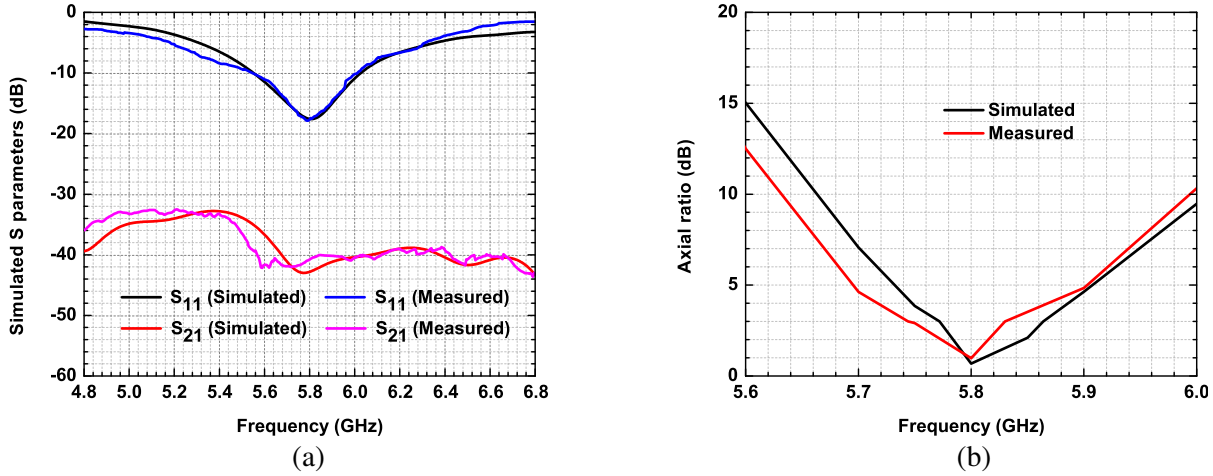

Figure 4. Comparison of (a) S parameters, and (b) axial ratio of proposed MIMO. (a) Simulated and measured S parameters. (b) Axial ratio.

Table 3. Frequency bands, isolations and AR bandwidth of proposed CP MIMO antenna.

No.	Frequency band (GHz)	Bandwidth (MHz) (−10 dB)	S_{21} (dB) (in band isolation)	AR band (3 dB)	AR bandwidth (MHz)
1	5.49–6.024 (Simulated)	534	>33 dB	5.772–5.864 GHz	92.0
2	5.56–6.01 (Measured)	450	>34 dB	5.744–5.83 GHz	86.0

5.744–5.83 GHz (AR bandwidth equals 86 MHz), and provides gain of 5.23 dBi. A comparison between the simulated and measured ARs is shown in Fig. 4(b). The different frequency bands along with the values of isolations and AR are shown in Table 3.

The high value of isolation ($S_{21} = S_{12}$) between different ports is due to the design and placement of the MIMO radiating elements. The feed mechanism along with the slot above the feed line and split in ground results in more than 33 dB of isolation between the radiating elements/ports. The two arms of feeder has $\lambda/2$ wavelength of separation to make proper operation of radiating elements. However, to limit the inter element coupling between two arms of the feeding network, a slot is etched in the ground plane just above the feed line, and also a ground split is used to limit direct coupling of MIMO radiators. Thus due to these approaches, lower value of surface current is concentrated on the non-excited port. As observable from Fig. 5, most of the current concentrates on the feed line and on the radiating elements of the excited port, and very less current is visible on the elements of non-excited port. The same concept is followed when the other port is excited. The scale shows different colors and corresponding values of current linked to the ports under different states. Similarly, when both ports are in excited state, a large value of current is concentrated on each of the excited ports and on their radiating elements.

The effect of slot above the feed line enhances the isolation by 3.44 dB at resonant. A comparison of S parameters and AR is carried out in Fig. 6(a) and Fig. 6(b). The proposed MIMO antenna with no slot above the feed line shows −10 dB impedance band of 5.5–6.018 GHz with more than 33 dB of in-band isolation and better return loss characteristics, and resonates at 5.816 GHz frequency with 38.25 dB of isolation at resonant. However, the antenna without a slot above the feed line has AR value greater than 6 dB, which means that the antenna is no longer in CP polarization. On the other hand, the proposed MIMO antenna with a slot above the feed line shows −10 dB impedance band of 5.49–6.024 GHz with more than 33 dB of in-band isolation. In this case, antenna resonates at 5.8 GHz

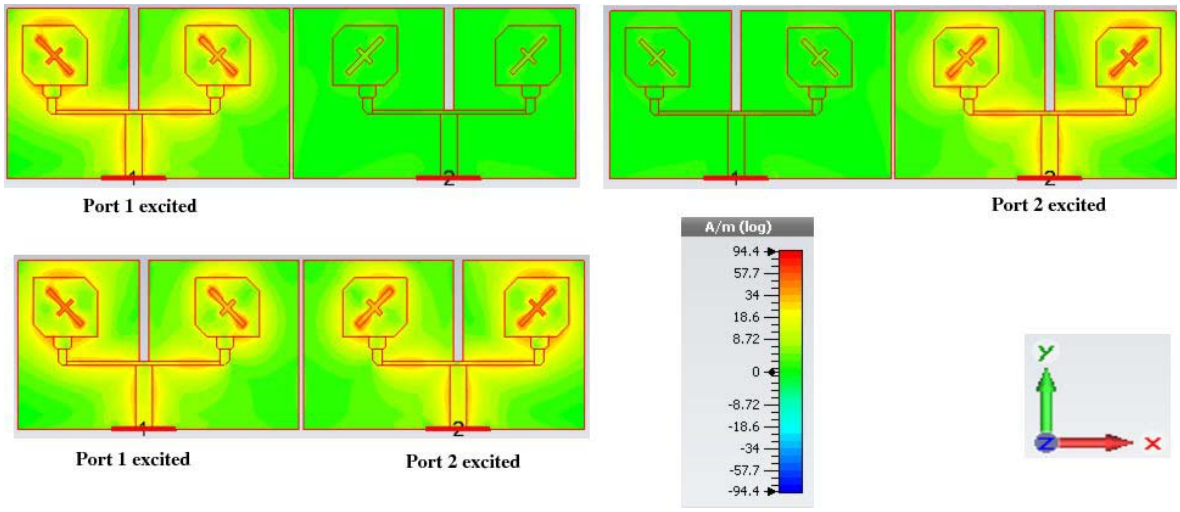

Figure 5. Surface current distribution of proposed 2 × 2 MIMO antenna.

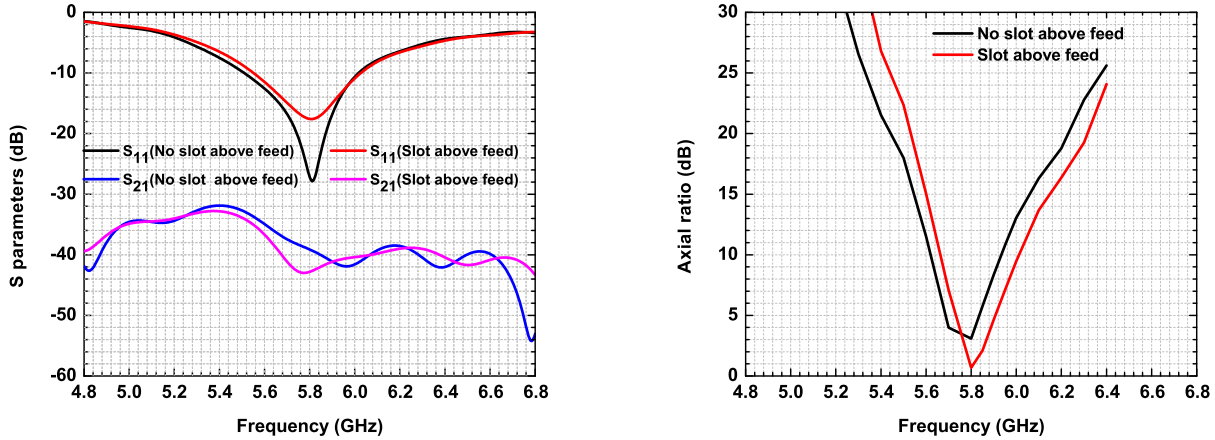

Figure 6. Comparison of S parameters and axial ratio (with and without the slot above the feed line). (a) Simulated S parameters. (b) Simulated axial ratio.

frequency with 42.82 dB of isolation and AR value of 0.68 dB, 3 dB AR band of 5.772–5.864 GHz (AR bandwidth equals 92.0 MHz), and gain of 5.34 dBi. Therefore, the presence of the slot above the feed line has a positive impact on CP polarization and also on the isolation.

Similarly, the effect of the phase difference (θ_1^0) between the major and minor slots can be seen on AR and voltage standing wave ratio (VSWR). The considered phase difference between these asymmetric slots is 90°. When θ_1^0 is varied from 0° to 90°, we observe that for 0° phase difference, both slots are merged, and only a major slot is seen. In this case, the value of AR is 1.95 dB, and VSWR has a value of 1.11. Similarly, when both the slots are 90° in phase difference, the value of AR is 0.68 dB, and VSWR has a value of 1.12. Similarly, for 45° phase difference, MIMO antenna has AR value of 40 dB and VSWR of 2.57. A major difference of AR values is observable here at 5.8 GHz resonant frequency. Therefore, we may state that for 0° and 90° of phase difference between the two slots, the proposed MIMO shows CP characteristics. For the other values of θ_1^0, the antenna has linear polarization. Therefore, the considered asymmetric slot case is better than the other cases. All the values have been plotted in Fig. 7 for the validity of proposed design.

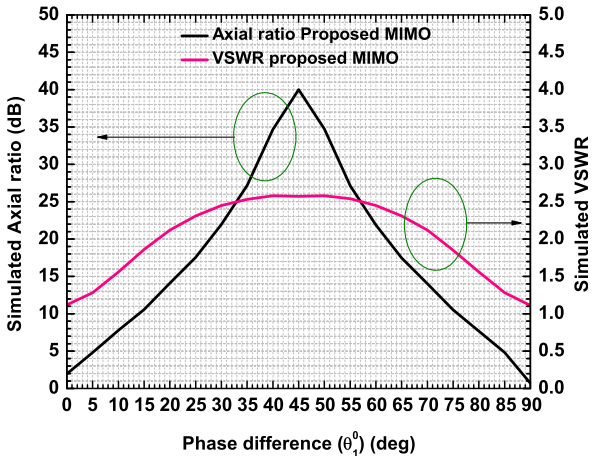

Figure 7. Effect of phase difference on proposed MIMO.

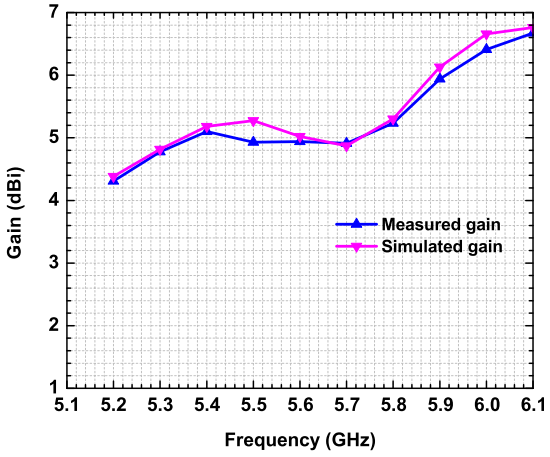

Figure 8. Gain of proposed MIMO antenna.

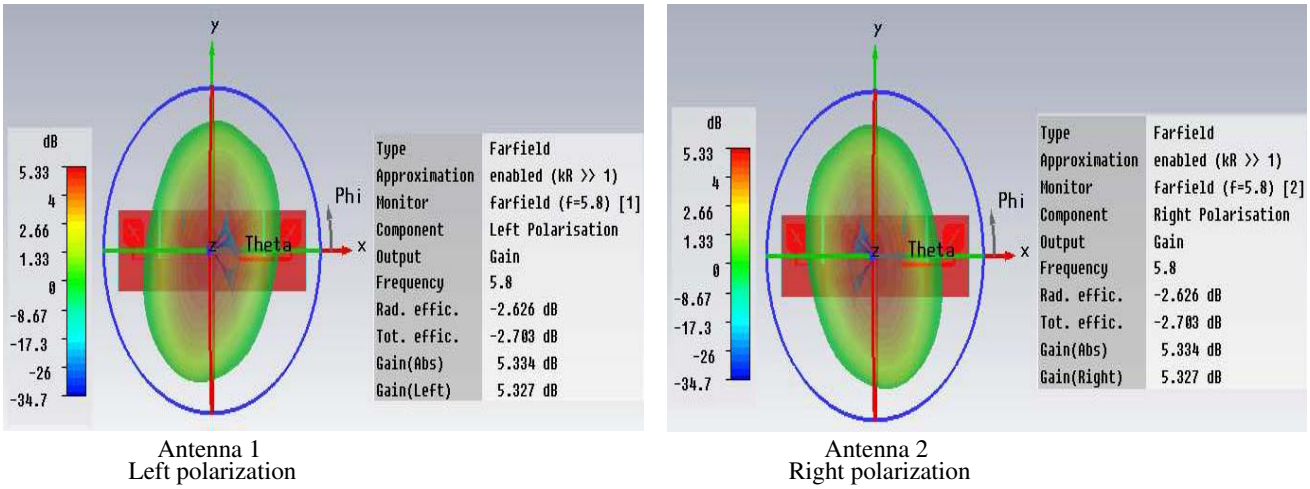

Figure 9. Left and right polarization patterns at 5.8 GHz for proposed MIMO.

2.2. Diversity Performance

The gain, envelope correlation coefficient (ECC), and mean effective gain (MEG) are used to describe the diversity behavior of the proposed 2×2 CP MIMO antenna here. The gain is a far-field parameter and measured in an anechoic chamber using the substitution method with two standard horn antennas and with the proposed MIMO antenna. The simulated gain of the proposed 2×2 CP MIMO antenna at 5.8 GHz resonant frequency is 5.34 dBi. Similarly, for the designed 2×2 CP MIMO, the measured value of gain at 5.8 GHz resonant frequency is 5.23 dBi. The simulated and measured gain values are plotted in Fig. 8 for all the frequencies. The corresponding left polarization of antenna 1 and right polarization of antenna 2 are shown in Fig. 9, for the effectiveness of the proposed design.

Similarly, the envelope correlation coefficient (ECC) also shows the diversity behavior of the proposed MIMO antenna. The isolation parameters S_{12} and S_{21} show only the information about the coupling at the ports. However, ECC involves all the scattering parameters of the proposed MIMO to show their effects on the correlation coefficient. Lowering the value of ECC means less correlation between antenna elements, while higher values of it shows the negative impact. For good diversity behavior, the value of ECC must be less than 0.5 for mobile applications. The simulated/measured values of ECC [25] may be obtained using the formula shown in Equation (1). Here the values of $i = 1$

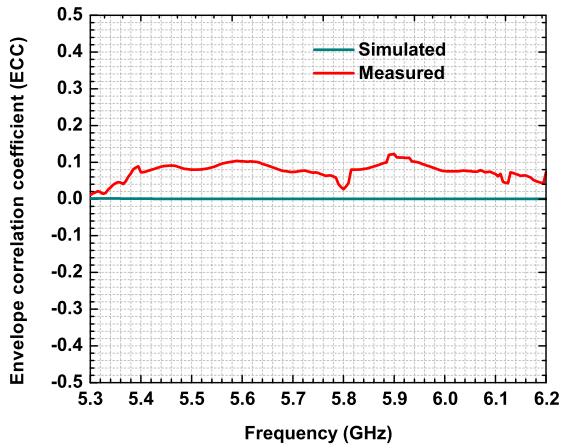

Figure 10. ECC of proposed MIMO antenna.

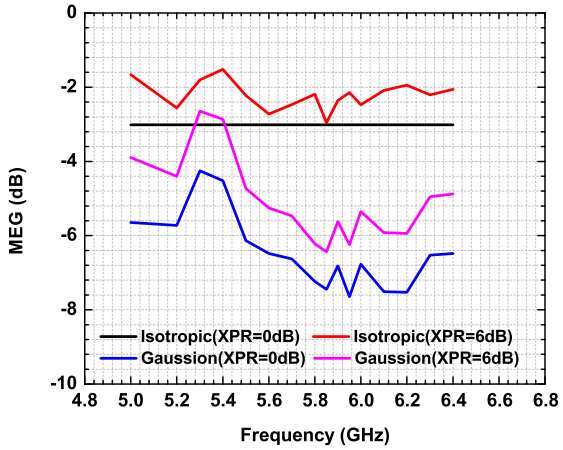

Figure 11. MEG of proposed MIMO antenna.

to 2 and $j = 1$ to 2 are for two elements, and $N = 2$ (as total 2 antennas).

$$|\rho_e(i,j,N)| = \frac{\left|\sum_{n=1}^{N} S_{i,n}^{*} S_{n,j}\right|}{\sqrt{\left|\prod_{k(=i,j)}\left[1 - \sum_{n=1}^{N} S_{i,n}^{*} S_{n,k}\right]\right|}} \tag{1}$$

As observable from Fig. 10 that the simulated values of ECC lies between the range of 0–0.0005 (due to very low values, it looks close to zero) in the whole frequency band, while the measured values of ECC between the two radiators lies in the range of 0–0.15. The simulated value of ECC at 5.8 GHz resonant frequency is 2.39×10^{-7}, and the corresponding measured value of ECC is 2.6×10^{-2}. The measured results showed fluctuation in ECC values, though we obtained very low ECC values between the two radiators at resonance and also in whole band. The big difference in the measured and simulated ranges/values is due to fabrication errors and port/cable coupling losses.

Similarly, the MEG is also a far-field parameter and is used to show diversity behavior. The MEG [26] includes power patterns of the proposed MIMO antenna. Let the cross polarization ratio be XPR, and the gaussian/uniform medium signals mean $(\mu) = 0$ and variance $(\sigma) = 20$, for both horizontal and vertical components. These two mediums (isotropic and gaussian/uniform mediums) have been considered for the analysis of the proposed MIMO antenna, for different values of XPR using CST simulations. Here, it has been observed that the values of MEG for isotropic medium with XPR = 0 dB show almost constant values of −3.5 dB, and with XPR = 6 dB MEG lie in the range of −1.6 to −3.5 dB. Similarly, the values of MEG for Gaussian medium with XPR = 0 dB lie in the range of −4.3 to −6.5 dB, and with XPR = 6 dBMEG lie in the range of −2.7 to −4.9 dB. All the values of MEGs are plotted in Fig. 11 for isotropic and gaussian mediums. A comparison of different simulated MEG values at 5.8 GHz resonant is shown in Table 4.

Table 4. MEG comparison of proposed 2 × 2 MIMO antenna at resonant.

Frequency (GHz)	MEG (Isotropic medium)		MEG (Gaussian medium)	
	XPR = 0 dB	XPR = 6 dB	XPR = 0 dB	XPR = 6 dB
5.8	−3.0	−2.25	−7.5	−6.46

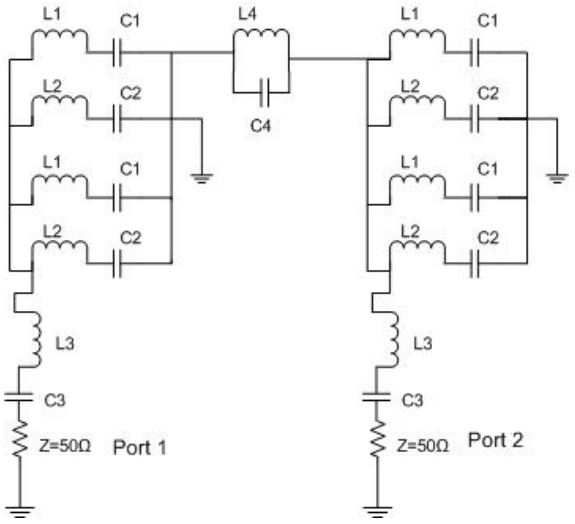

Figure 12. Equivalent circuit model.

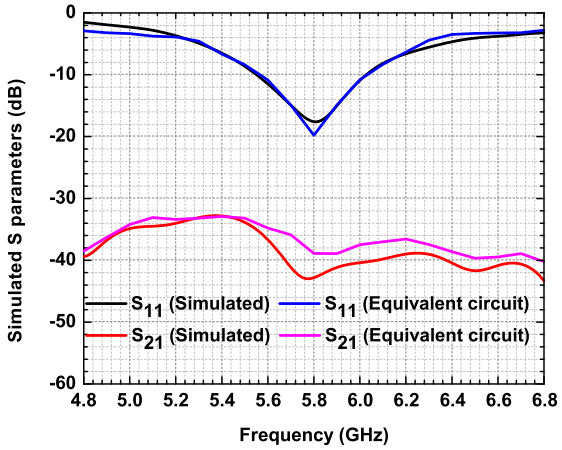

Figure 13. Comparison of S parameters.

2.3. Equivalent Circuit Modeling

For the cross verification of resonant property of the proposed 2×2 CP MIMO antenna, an equivalent circuit model was developed using advanced system design (ADS)-2016. This in turn cross verifies the effect of tuning behavior of each patch, slot, and discontinuities (combination of two different wavelength transmission lines). These are modeled as a combination of inductor (L) and capacitor (C). Each of the ports is replaced by a $50\,\Omega$ load. Each of the patches is modeled using series combination of $L1$ and $C1$, and the effect of two asymmetric slots by the series combination of $L2$ and $C2$. Similarly, the combination of $50\,\Omega$, $70.7\,\Omega$, and $100\,\Omega$ microstrip transmission lines is jointly represented by series combination of $L3$ and $C3$, and the coupling effect between the two ports is modeled as a parallel combination of $L4$ and $C4$. The corresponding values of these elements as $L1 = 1.2\,\text{nH}$, $L2 = 0.66\,\text{nH}$, $L3 = 0.9\,\text{nH}$, $L4 = 1.99\,\text{nH}$, $C1 = 0.86\,\text{pF}$, $C2 = 0.76\,\text{pF}$, $C3 = 0.6\,\text{pF}$, $C4 = 0.9\,\text{pF}$ were simulated using ADS software. The equivalent model is shown in Fig. 12. The corresponding responses (S_{11} and S_{21}) are compared with the CST simulated responses in Fig. 13. The responses using equivalent resonant circuit and CST full wave simulation are very similar for the return loss and isolation parameters.

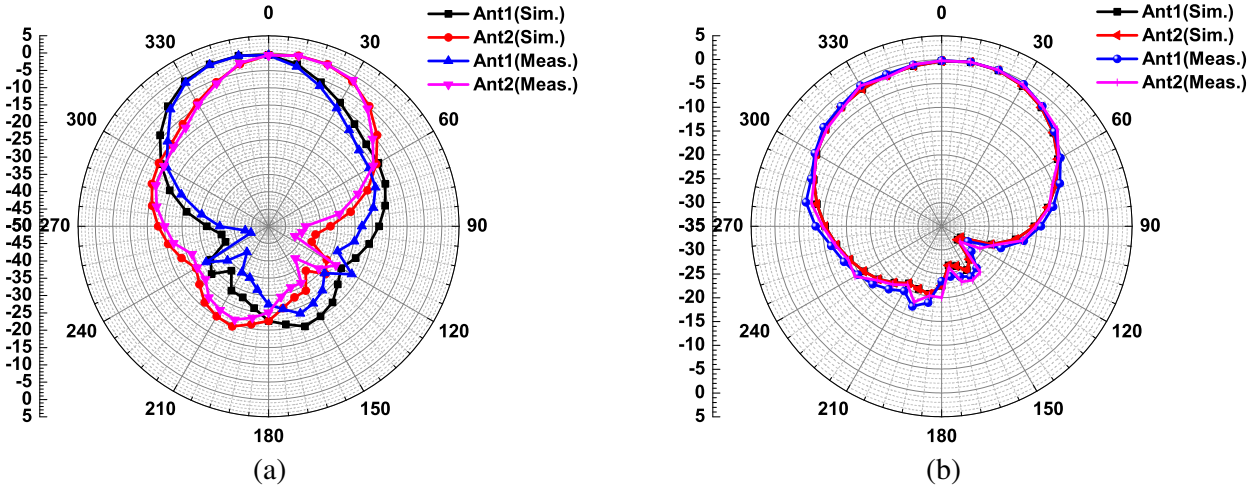

Figure 14. E and H field radiation patterns of proposed CP MIMO at 5.8 GHz. (a) E field radiation patterns. (b) H field radiation patterns.

2.4. Far Field Radiation Patterns

The far-field radiation patterns of the proposed 2×2 CP MIMO antenna are measured in an anechoic chamber at 5.8 GHz resonant frequency for E and H field patterns, for each of the port. The instruments/devices required in the anechoic chamber are standard horn antenna (used as a transmitting antenna), microwave generator, power meter, and fabricated 2×2 CP MIMO antenna. When any one of the port is used in receiving mode, the other port is terminated by 50 Ω to avoid any noise pick-up.

The proposed 2×2 CP MIMO antenna elements are mirrored to have balanced radiation patterns and also to avoid mismatching. The E field radiation patterns have main lobe directions of $\pm 10^\circ$, and the angular widths are 57.6°. Similarly, the H field radiation patterns also have main lobe directions of $\pm 10^\circ$, and the angular widths are 92.5°. The measured and simulated E and H field patterns are compared in Fig. 14(a) and Fig. 14(b).

3. CONCLUSION

A compact CP MIMO antenna with power divider was proposed for 5.8 GHz WLAN standards using two optimized 90° apart rectangular slots. Various aspects of MIMO antenna were discussed in this paper for the effectiveness of design on S parameters and axial ratio. The proposed MIMO covered 5.49–6.024 GHz frequency band with more than 33 dB of isolation between ports and better AR characteristics. Also the measured ECC was around 0.15, very much less than the maximum limit set for wireless communication.

REFERENCES

1. Rezaeieh, A. S., S. Simsek, and J. Pourahmadazar, "Design of a compact broadband circularly polarized slot antenna for wireless applications," *Microwave and Optical Technology Letters*, Vol. 55, No. 2, 413–418, 2013.
2. Gautam, A. K. and B. K. Kanaujia, "A novel dual-band asymmetric slit with defected ground structure microstrip antenna for circular polarization operation," *Microwave and Optical Technology Letters*, Vol. 55, No. 6, 1198–1201, 2013.
3. Kumar, S., B. K.. Kanaujia, A. Sharma, M. Khandelwal, and A. K. Gautam, "Single feed cross slot loaded compact circularly polarized microstrip antenna for indoor WLAN applications," *Microwave and Optical Technology Letters*, Vol. 56, No. 6, 1313–1317, 2014.
4. Abraham, J., T. Mathew, and C. K. Aanandan, "A novel proximity fed gap coupled microstrip patch array for wireless applications," *Progress In Electromagnetic Research C*, Vol. 61, 171–178, 2016.
5. Khawaja, B. A., M. A. Tarar, T. Tauqeer, F. Amir, and M. Mustaqim, "A 1×2 triple band printed antenna array for use in next generation flying Ad-hoc networks," *Microwave and Optical Technology Letters*, Vol. 58, No. 3, 606–610, 2016.
6. Yu, A., F. Yang, and A. Z. Elsherbeni, "A planar rhombic antenna with a broad circular polarization bandwidth for integrated single chip radio receivers," *Microwave and Optical Technology Letters*, Vol. 51, No. 6, 1493–1496, 2009.
7. Rao, P. N. and N. V. S. N. Sharma, "Compact single feed circularly polarized fractal boundary microstrip antenna," *Microwave and Optical Technology Letters*, Vol. 52, No. 1, 141–147, 2010.
8. Bilgic, M. M. and K. Yegin, "Wideband high gain aperture coupled antenna for Ku band phased array systems," *Microwave and Optical Technology Letters*, Vol. 55, No. 6, 1291–1295, 2013.
9. Jiang, Y., G. Wen, and H. Sun, "A new focused antenna array with circular polarization," *Microwave and Optical Technology Letters*, Vol. 57, No. 12, 2936–2939, 2015.
10. Karamzadeh, S., B. S. Virdee, V. Rafii, and M. Kartal, "Circularly polarized slot antenna array with sequentially rotated feed network for broadband application," *International Journal of RF and Microwave Computer Aided Engineering*, Vol. 25, No. 4, 358–363, 2015.
11. Al-Ajmi, A. R. and S. F. Mahmoud, "A single feed circularly polarized patch antenna for reduced surface wave applications," *Microwave and Optical Technology Letters*, Vol. 51, No. 11, 2675–2679, 2009.

12. Sun, C., H. Zheng, and Y. Liu, "Analysis and design of a low cost dual-band compact circularly polarized antenna for GPS application," *IEEE Transactions on Antennas and Propagation*, Vol. 64, No. 1, 365–370, 2016.
13. Chen, H. M., K. Y. Chiu, Y. F. Lin, and S. A. Yeh, "Circularly polarized slot antenna design and analysis using magnetic current distribution for RFID reader applications," *Microwave and Optical Technology Letters*, Vol. 54, No. 9, 2016–2022, 2012.
14. Yang, J., C. H. Liang, and T. Wang, "Novel dual-band circularly polarized wideband antenna for WLAN and WiMAX," *Journal of Electromagnetic Waves and Applications*, Vol. 26, Nos. 14–15, 1881–1888, 2012.
15. Lai, X.-Z., Z.-M. Xie, and X.-L. Cen, "Design of a dual circularly polarized antenna with high isolation for RFID applications," *Progress In Electromagnetics Research*, Vol. 139, 25–39, 2013.
16. Huang, W., L. Sun, B. Sun, and Q. Sun, "Circularly polarized magnetic dipole with shallow and embedded structure for airborne GPS applications," *Microwave and Optical Technology Letters*, Vol. 57, No. 4, 902–906, 2015.
17. Mondal, T., S. Samanta, R. Ghatak, and S. R. B. Chaudhuri, "A novel hexagonal wideband circularly polarized stacked patch microstrip antenna," *Microwave and Optical Technology Letters*, Vol. 57, No. 11, 2548–2554, 2015.
18. Wang, J., Z. Lv, and X. Li, "Analysis of MIMO diversity improvement using circular polarized antenna," *International Journal of Antennas and Propagation*, Vol. 2014, 1–9, 2014.
19. Gang, L. J., G. X. Jun, and Z. H. Zhou, "The design of broadband circularly polarized planar microstrip antenna array," *Microwave and Optical Technology Letters*, Vol. 49, No. 12, 2936–2939, 2007.
20. Nayan, M. K. A., M. F. Jamlos, and M. A. Jamlos, "Circularly polarized MIMO antenna array for point to point communication," *Microwave and Optical Technology Letters*, Vol. 57, No. 1, 242–247, 2015.
21. Nayan, M. K. A., M. F. Jamlos, and M. A. Jamlos, "MIMO circular polarization array antenna with dual coupled 90° phased shift for point to point applications," *Microwave and Optical Technology Letters*, Vol. 57, No. 4, 809–814, 2015.
22. Nayan, M. K. A., M. F. Jamlos, H. Lago, and M. A. Jamlos, "Two port circular polarized antenna array for point to point applications," *Microwave and Optical Technology Letters*, Vol. 57, No. 10, 2328–2332, 2015.
23. Lu, J. H. and Y. H. Liu, "Novel dual-band design of planar slot array antenna for 4G LTE/WiMAX access points," *Microwave and Optical Technology Letters*, Vol. 54, No. 5, 1193–1196, 2012.
24. Haghparast, A. H. and G. Dadashzadeh, "A dual-band polygon shaped CPW-fed planar monopole antenna with circular polarization and isolation enhancement for MIMO applications," *9th European Conference on Antennas and Propagation (EuCAP)*, 1–4, 2015.
25. Sharawi, M. S., M. A. Jan, and D. N. Aloi, "Four shaped 2×2 multi standard compact multiple input multiple output antenna system for long term evolution mobile handsets," *IET Microwaves Antennas and Propagation*, Vol. 5, No. 7, 685–696, 2012.
26. Taga, T., "Analysis for mean effective gain of mobile antennas in land mobile radio environments," *IEEE Transactions on Antennas and Vehicular Technology*, Vol. 39, No. 2, 954–960, 2001.